Journal of Applied Polymer Science

Solvent-free synthesis of polyols from 1-butene metathesized palm oil for use in polyurethane foams

Prasanth K. S. Pillai,[1,2] Shaojun Li,[1,2] Laziz Bouzidi,[1,2] Suresh S. Narine[1,2]

[1]Trent Centre for Biomaterials Research, Department of Physics and Astronomy, Trent University, 1600 West Bank Drive, Peterborough Ontario, CanadaK9J 7B8

[2]Trent Centre for Biomaterials Research, Department of Chemistry, Trent University, 1600 West Bank Drive, Peterborough Ontario, CanadaK9J 7B8

Correspondence to: S. S. Narine (E-mail: sureshnarine@trentu.ca)

ABSTRACT: Green Polyols were synthesized from a 1-butene cross metathesized palm oil (PMTAG) using a green, solvent free epoxidation and hydroxylation pathway. The synthetic strategy was adapted to control the degree of double bond epoxidation and ultimately the hydroxyl value of the polyols. The polyols comprised diol and tetrol monomers with terminal hydroxyl groups content as high as ~18 mol %, and achieved hydroxyl values between 83 and 119 mg KOH g^{-1}. Functional Rigid and highly flexible foams were prepared from two designer Green Polyols. The foams presented a high thermal stability (T_{on} of degradation of ~270 °C), suitable glass transition temperatures (~−12 °C and ~50 °C) and compressive strength (0.21 MPa at 10% strain and ~1 MPa at 10% strain for the flexible and rigid foams, respectively) which are superior to existing lipid-based counterparts. © 2016 Wiley Periodicals, Inc. J. Appl. Polym. Sci. **2016**, *133*, 43509.

KEYWORDS: biopolymers and renewable polymers; foams; metathesis

Received 22 October 2015; accepted 3 February 2016

DOI: 10.1002/app.43509

INTRODUCTION

Polyurethanes (PU) are versatile polymers which have traditionally been manufactured from petroleum.[1] The range of polyurethane products includes polyurethane elastomers,[2] sheets,[2] adhesives,[3] coatings,[4] and foams,[2] spanning uses across a large array of industries and products. With a market of $82.6 billion in 2012, PU foams have the largest market share of polymers, projected to reach $131.1 billion by 2018.[5] PU can be prepared via two principal routes, in the step growth polymerization of isocyanate (NCO) groups and hydroxyl groups[6] and with non-isocyanate pathways, such as the reaction of cyclic carbonates with amines,[7] self-polycondensation of hydroxyl-acyl azides or melt transurethane methods.[8]

Growing concerns surrounding sustainability, biodegradability, control of CO_2 emissions, and other environmental problems are driving a search for alternative feedstock to petroleum. Vegetable oils and their derivatives are seen as good renewable materials for the synthesis of polymer substrates, particularly for polyols used in PU production. A considerable body of work has been already published related to the synthesis of polyols and polyurethanes from a variety of vegetable TAG oils such as soybean oil,[9,10] safflower oil, corn oil, sunflower seed oil, linseed oil,[11] rapeseed oil,[12] and cotton seed oil.[13]

Palm oil presents a particularly interesting potential for industrial use as it is one of the least expensive and most widely available oils (53 million metric ton in 2013: according to the FAO).[14] However, its high saturated fatty acid composition (50% of the total) and the internal nature of its double bonds limit the potential use of palm oil in PU foam formulations, particularly in rigid PU foams.[15,16] The internal location of the double bonds results in polyol functionalization with secondary hydroxyl groups, which are less reactive and lead to incomplete crosslinking during polymerization and imperfections in the polymer network.[2,16] The regions where dangling chains are present do not support stress when the sample is under force, and act as plasticizers, reducing polymer rigidity.[15,16]

Olefin cross metathesis of natural oils and fats is an important organic synthesis technique that is used to produce fine chemicals, substrates, and materials, many of which serve as or are potential petrochemical replacements.[16–20] The cross metathesis reaction effectively shortens some of the unsaturated fatty acids of the TAGs at the unsaturated sites, producing terminal double

Additional Supporting Information may be found in the online version of this article.

bonds,[21,22] which gives the potential of producing polyols with primary hydroxyl groups, and therefore dramatically reduces dangling chains in polyurethane networks.[16,23] In addition, the composition of a metathesized product can be controlled by varying the reaction conditions, such as starting materials, temperature, type of catalyst, etc.[24–26] allowing for a large range of designer materials.

The present work is part of research efforts targeted at investigating the potential of metathesized vegetable oil products for the production of polyols for PU and other polymer applications, and other useful materials. The starting material used in the present study is a 1-butene cross metathesized palm oil (PMTAG) stripped of its olefins, provided by Elevance Renewable Science (ERS). Its full chemical and physical characterization and its conversion into polyols, using solvent-mediated processes, for the preparation of rigid and flexible polyurethane foams have already been reported.[27] Previously, polyols were produced from PMTAG using epoxidation reactions, followed by a hydroxylation method and involved the utilization of harsh and dangerous solvents like DCM and THF.

The present effort was targeted at the synthesis of polyols from PMTAG using green, one pot solvent free epoxidation and hydroxylation pathways. The synthesis of green polyols from soybean oil and castor oil by solvent free/catalyst free epoxidation for polyurethane applications was previously reported.[28] The solvent free synthetic route is not only safer and environmentally friendly, but also much more economical. The epoxidation and hydroxylation reaction conditions were tuned to control the conversion of PMTAG double bonds into hydroxyl groups and hence control the hydroxyl value of the polyols. Four batches (B1-4) of these so-called Green Polyols were produced. The chemical structure and composition of the polyols were characterized by ^{1}HNMR, HPLC, OH value, and Iodine value. Thermal stability, thermal transition behavior, and flow properties were determined by TGA, DSC, and rotational rheometry, respectively. Rigid and a flexible foams were prepared from the Green Polyols with OH values of 83 and 119 mg KOH g^{-1}, respectively. The foams were characterized by FTIR and SEM. Their thermal stability, thermal transition behavior, and compressive strength were investigated using TGA, DSC, and a texture analyzer, respectively.

EXPERIMENTAL

Materials

PMTAG was provided by Elevance Renewable Sciences (ERS, Bolingbrook, II). Formic acid (88 wt %), Iodine monochloride (95%), potassium iodide (99%), phenolphthalein, hydrogen peroxide solution (30 wt %), Dibutin Dilaurate (DBTDL) and glycerin (99.5%) were purchased from Sigma–Aldrich, Canada (Oakville, Ontario, Canada). Perchloric acid (70%) and *N*,*N*-dimethylethanolamine (DMEA were purchased from Fisher Scientific, Canada. Ethanol (anhydrous), toluene, potassium hydroxide, and sodium thiosulfate were purchased from ACP chemical (Montreal, Quebec, Canada). All of the above compounds were used as received. Diphenylmethane diisocynate (MDI) from Baer Materials Science (Pittsburgh, PA), Polyether-modified surfactant (TEGOSTAB B-8404) from Goldschmidt Chemical Canada. The properties of the MDI are presented in Table SI in the Supporting Information.

Chemistry Characterization

Titrimetric Methods (OH Value, Acid Value, Iodine Value). OH and acid values of the PMTAG Polyol were determined according to ASTM S957-86 and ASTM D4662-03, respectively. Iodine value was determined according to ASTM D5768-02.

Proton Nuclear Magnetic Resonance Spectroscopy (^{1}HNMR). ^{1}H NMR spectra were recorded in $CDCl_3$ on a Varian Unity-INOVA at 499.695 MHz. All spectra were obtained using an 8.6 μs pulse with four transients collected in 16,202 points. Datasets were zero-filled to 64,000 points, and a line broadening of 0.4 Hz was applied prior to Fourier transformation. The spectra were processed using spinwork NMR Processor, version 3. ^{1}H chemical shifts are internally referenced to $CDCl_3$ (7.26 ppm).

Gel Permeation Chromatography (GPC). Molecular weights and distribution were determined by gel permeation chromatography (GPC). The measurements were carried out on an e2695 GPC instrument equipped with a Waters e2695 pump, Waters 2414 refractive index detector and a 5-μm Styragel HR5E column (Waters Alliance, Milford, MA). Chloroform was used as eluent with a flow rate of 0.5 mL min^{-1}. The concentration of sample was 1 mg mL^{-1} and the injection volume was 10 μL. Polystyrene (PS) standards and pure TAG-oligomers (synthesized previously[29]) were used for calibration. Waters Empower Version 2 software was used for data collection and data analysis.

Fourier Transform Infrared Spectroscopy (FTIR). The FTIR spectra of the foams were obtained with a Thermo Scientific Nicolet 380 FTIR spectrometer (Thermo Electron Scientific Instruments, LLC, USA) equipped with a PIKE MIRacle^{TM} attenuated total reflectance (ATR) system (PIKE Technologies, Madison, WI). Solid samples were loaded onto the ATR crystal area, and sample spectra were acquired over a scanning range of 400–4000 cm^{-1} for 32 repeated scans at a spectral resolution of 4 cm^{-1}.

Physical Characterization Techniques

Thermogravimetric Analysis (TGA). TGA measurements were carried out on a TGA Q500 (TA Instruments, DE, USA) equipped with a TGA heat exchanger (P/N 953160.901). Approximately 8.0–15.0 mg of sample was loaded into the open TGA platinum pan. The sample was heated at a constant rate of 10 °C/min from 25 to 600 °C under dry nitrogen. The "TA Universal Analysis" software (TA Instruments, New Castle, DE) was used to analyze the TGA curves.

Differential Scanning Calorimetry (DSC). DSC measurements were performed on a Q200 model (TA Instruments, New Castle, DE) under a nitrogen flow of 50 mL min^{-1}.

Polyol samples between 3.5 and 6.5 ($\pm$ 0.1) mg were run in standard mode in hermetically sealed aluminum pans. The sample was equilibrated at 90 °C for 10 min to erase thermal memory, and then cooled at 5.0 °C min^{-1} to −90 °C where it was held isothermally for 5 min and subsequently reheated at a 5.0 °C min^{-1} to 90 °C.

Foam samples between 3.0 and 6.0 (± 0.1) mg were run in modulated mode in hermetically sealed aluminum DSC pans. The sample was first equilibrated at 25 °C and heated to 150 °C at 10 °C min^{-1} (first heating cycle). The sample was held at that temperature for 10 min and then cooled to −90 °C at 10 °C min^{-1}, where it is held isothermally for 5 min and subsequently reheated to 150 °C at the same rate (second heating cycle). The modulation amplitude and period were ±1 °C and 60 s, respectively.

The "TA Universal Analysis" software was used to analyze the DSC thermograms. The characteristics of non-resolved peaks were obtained using the first and second derivatives of the differential heat flow.

Rheology. The flow behavior and viscosity versus temperature of the polyols were measured on a temperature controlled Rheometer (AR2000ex) using a 40-mm, 2° steel geometry. Temperature control was achieved by a Peltier attachment with an accuracy of ~0.1 °C. Shear stress versus shear rate curves were measured at 10 °C intervals from high temperature (100 °C) to ~10 °C below the DSC onset of crystallization temperature. The viscosity versus temperature data were collected at constant shear rate (200 s^{-1}) using the ramp procedure while the sample was cooling (1.0 and 3.0 °C min^{-1}) from ~110 °C to just above the crystallization point. Data points were collected at 1 °C intervals.

The shear rate–shear stress curves were fitted with the Herschel–Bulkley equation [eq. (1)], a model commonly used to describe the general flow behavior of liquid materials, including those characterized by a yield stress.

$$\tau = \tau_0 + K\dot{\gamma}^n \quad (1)$$

Where $\dot{\gamma}$ denotes the shear stress, τ_0 is the yield stress below which there is no flow, K the consistency index and n the power index. n depends on constitutive properties of the material. For Newtonian fluids $n = 1$, and for shear thickening and shear thinning fluids $n > 1$ and $n < 1$, respectively.

Texture Analysis. The compressive strength of the foams was measured at room temperature using a texture analyzer (TA-TX HD, Texture Technologies Corp, NJ). Samples were prepared in cylindrical Teflon molds 60-mm in diameter and 36-mm in length. During compressive force measurements, the cross head speed was 3.54 mm min^{-1}, recorded on a 750 Kgf load cell for both the rigid and flexible foams. The load was applied until the foam was compressed to ~15 and 65% of the original thickness of the rigid and flexible foams, respectively.

Scanning Electron Microscopy (SEM). Composite SEM images of the foams were resolved with a Phenom ProX, (Phenom-World, The Netherlands) scanning electron microscope at an accelerating voltage of 15 kV and map intensity. Uncoated foams were cut into thin rectangular segments and fixed to a temperature controlled sample holder with conductive tape. Samples were cooled to −25 °C to prevent beam induced thermal deformations, and composite images were captured using the Automated Image Mapping software (Phenom-World, The Netherlands).

Table I. Epoxidation Reaction Temperature and Time Data for the Synthesis of Green Polyols

	Epoxidation			
Batch	T_{ini}^{Epx}	T_{max}^{Epx}	T_{R}^{Epx}	t_{R}^{Epx}
1	50	65	48	16 h at 45 °C then 12 h at 48 °C
2	40	49	48	16h at 48 °C
3	25	95	45	16h at 45 °C
4	25	48	25	16h at 25–48 °C

T_{ini}^{Epx}: Initial temperature of the epoxidation reaction; T_{max}^{Epx}: highest temperature reached during the epoxidation reaction; T_{R}^{Epx}: reaction temperature for epoxidation; t_{R}^{Epx}: reaction time.

Synthesis Methods

Epoxidation. The 2 kg PMTAG was added into 2 kg formic acid (88%) in a 20L reactor fitted with a HAAKE Phoenix II temperature controlled circulator (Thermoscientific, Newington, NH). The initial reaction temperature of the epoxidation was varied (T_{ini}^{Epx} in Table I) depending on the batch. 2.8 L of hydrogen peroxide (30%) was added to the reactor slowly (~1 L h^{-1}) while the reaction mixture was vigorously stirred. During addition of hydrogen peroxide, the exothermic nature of the epoxidation reaction caused the temperature to increase. In the case of Batch 3, the temperature controlled system wasn't used; the temperature of the reaction reached a maximum of 95 °C but remained less than 10 min at that temperature. Because of the exothermic nature of the epoxidation reaction, the temperature of the other batches also increased (T_{max}^{Epx} in Table I). Tap water was circulated to cool Batch 4, and the control feature of the circulator was used to bring Batch 1 and Batch 2 to the actual epoxidation temperature (T_{R}^{Epx} in Table I). The epoxidation reaction was continued at T_{R}^{Epx} overnight. The reaction mixture was finally washed with 2 × 1 L water, 1 × 1 L 5% $NaHCO_3$ and 2 × 1 L water sequentially. The mixture was used for the next step directly. Yield > 95%.

Hydroxylation. The epoxide of PMTAG (2 kg) above was added into 10 L water, and then followed by 140 g $HClO_4$ (70%) with a ratio of PMTAG/H_2O/perchloric acid = 1/5/0.05. The reaction mixture was heated to ~85 °C and stirred at that temperature for 16 h after which stirring and heat were ceased and the mixture sat at room temperature to aid in separation. The organic layer was washed with 2 × 1 L water, 1 × 1 L 5% $NaHCO_3$ and 2 × 1 L water sequentially, and then dried on a rotary evaporator. Yield > 95%.

Polymerization Method. Rigid and flexible polyurethane foams were prepared from B3- and B4-Green polyol and MDI using a previously published method.[2] The formulation recipes for the rigid and flexible foams are presented in Table II. The amount of each component was based on 100 polyol parts by weight. As shown in Table II, the rigid foams were prepared based on a total hydroxyl value of 450 mg KOH g^{-1}. In The case of the rigid foams, glycerin, a poly hydroxyl cross linker, was added into the reaction mixture (20.1 and 18.1 parts for B3- and B4-

Table II. Formulation Recipes for Rigid and Flexible Foams

Ingredient		Rigid foams Parts	Flexible foams Parts
B3-Green Polyol or B4-Green Polyol		100	100
OH:NCO ratio		1:1.2	1:1.2
Glycerin	B3	20.1	0
	B4	18.1	0
Water		2	2
Surfactant (Tegostab)		2	2
Cross linking catalyst (DBTDL)		1	0.5
Blowing catalyst (DMEA)		1	0.5

Amounts are based on 100 parts by weight of total polyol.

Polyol Rigid Foams, respectively) in order to obtain the targeted hydroxyl value of 450 mg KOH g^{-1} (see Table II).

The amount of MDI in both rigid and flexible foam formulations was adjusted to achieve an isocyanate index of 1.2 (NCO to OH ratio of 1.2 to 1) taking into account the contributions of the water and added.

The amount of cross linking catalyst DBTDL, which favors the gelling reaction, and the cocatalyst DMEA, which functions as a blowing catalyst, were fixed at 1 and 0.5 parts respectively based on the fairly good compressive strength previously obtained for rigid polyurethane foams prepared from terminal hydroxyl polyols.[2]

The crosslinking catalyst DBTDL, which favors the gelling reaction, and the cocatalyst DMEA, which functions as a blowing catalyst, were used for the polymerization process. The choice of the catalyst ratios were fixed based on the fairly good compressive strength previously obtained for rigid polyurethane foams prepared from terminal hydroxyl polyols.[2]

All the ingredients except MDI were melt and weighed into a beaker and hand mixed for 5–20 s. The pre-measured MDI was then added into the beaker and stirred vigorously by hand mixing for 8–20 s and transferred into a cylindrical Teflon mold (60-mm diameter and 35-mm long) which was previously greased with silicone release agent. The mold was then then sealed with a hand tightened clamp and the sample was cured for 4 days at 40 °C, with an additional post curing of 1 day at room temperature. Table II gives the formulation recipe used for the preparation of rigid and flexible polyurethane foams from B3- and B4-Green Polyols.

RESULTS AND DISCUSSION

Solvent Free Synthesis of Polyol from PMTAG

The Green Polyols were prepared from PMTAG in a solvent-free one-pot two-step reaction; epoxidation by formic acid and hydrogen peroxide (H_2O_2), followed by hydroxylation using perchloric acid ($HClO_4$) as the catalyst, as described in Scheme 1. The formic acid (88%)/H_2O_2 (30%)/PMTAG ratio was kept at 1/1.4/1 and PMTAG/H_2O/perchloric acid at 1/5/0.05 in all the batches. The epoxidation conditions (temperature and time)

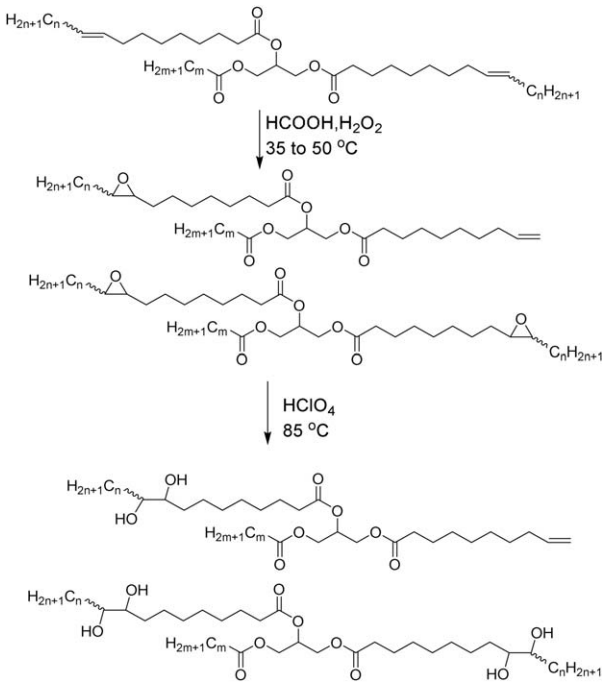

Scheme 1. Solvent-free synthesis of polyols from PMTAG. $n = 0, 2, 8$; $m = 11$ to 20.

were adjusted in order to optimize the reaction, control the OH value, and to manage the amount of formic acid that can become attached to the polyol. The temperature and time of the four different batches of epoxidation reactions were tuned so as to control the conversion of the double bonds into epoxides (see Table I). The controlled double bond conversion subsequently enables the production of polyols with controlled hydroxyl value. Note that when the temperature was below 70 °C, the degree of epoxidation in the melt was limited (~80 to 90% conversion of total double bonds). Also, at temperatures higher than 50 °C, the epoxide was opened by formic acid and formic acid units were found attached to some of the polyol backbones. Therefore, in order to avoid formic acid units attached to the polyol backbone, the epoxidation temperature should be kept below 50 °C. The hydroxylation of all the batches was run at 85 °C over 16 h. The Green Polyols obtained from the four batches are labelled B1–B4-Polyol.

Chemical Characterization and Compositional Analysis of PMTAG Green Polyols

The structure of the epoxides was confirmed by ^{1}H NMR. The characteristic chemical shift values of the specific protons of B1-, B2-, B3-, and B4-epoxy PMTAG are provided in the Supporting Information in Table SII. The chemical shift at 2.85 ppm, related to the nonterminal epoxy ring, and the chemical shift at 2.7–2.4 ppm related to the terminal epoxy ring appeared for the epoxidized PMTAG of all the batches, indicating that the epoxidation reaction was successful. However, although the chemical shift at 5.4 ppm related to internal double bonds disappeared; peaks at 5.0–4.8 ppm were still present, indicating that the terminal double bonds were not completely converted into epoxides.

Table III. Amount of Remaining Terminal Double Bonds (RTDB),[a] Number of Formic Acid Units per TAG Polyol and Terminal OH Groups as Estimated by ^{1}H NMR

	Green PMTAG epoxides		Green polyols					
Batch	RTDB (mol %)[a]	Formic acid units per TAG	RTDB (mol %)	Terminal OH group (mol %)	Iodine Value	OH value (mg KOH^{-1} g^{-1})	Acid value (mg KOH^{-1} g^{-1})	Functionality (±0.1)
B1	25.0	0.14	25.0	18.7	5	113	5	~3.2
B2	26.0	0.14	26.0	18.5	7	117	1.3	~3.2
B3	34.0	0.00	34.0	16.6	9	83	1.3	~3.0
B4	27.0	0.00	27.0	18.3	8	119	1.3	~3.2

Iodine value, acid value, and OH number of PMTAG Green Polyols.
[a] Remaining terminal double bonds (RTDB %) was calculated as the ratio of remaining terminal double-bonded fatty acids in Green Polyol to the terminal double bonded fatty acids in PMTAG.

The relative amount of remaining terminal double bonds (RTDB) as estimated by ^{1}H NMR for each batch of epoxy PMTAG is provided in Table III. Note that RTDB (mol %) was calculated as the ratio of remaining terminal double-bonds in the PMTAG epoxide to the terminal double bonds in the starting PMTAG material. The chemical shift at δ 8 ppm indicating the presence of formic acid attached to the backbone of the epoxide was present in the epoxidized PMTAG of B1 and B2 but not B3 and B4. The number of formic acid units per TAG epoxide, as estimated by ^{1}H NMR, is provided in Table III.

The structure of the Green Polyols (B1 to B4) was confirmed by ^{1}H NMR. Figure S1(a–d) in the Supporting Information show the ^{1}H NMR spectra of B1-B4 Green Polyols, respectively. The corresponding ^{1}H NMR chemical shifts in $CDCl_3$ are listed in Supporting Information Table SIII. The spectra of all the polyols presented the chemical shift related to protons neighbored by —OH (at 3.8–3.4 ppm) but not the chemical shift related to epoxy rings (at 2.8–2.4 ppm) indicating that the hydroxylation reaction was complete. The Green Polyols presented the typical chemical shift related to a glycerol skeleton: —$CH_2C\mathbf{H}(O)CH_2$— at δ 5.3–5.2 ppm, —$OC\mathbf{H}_2CH(O)C\mathbf{H}_2O$— at 4.4–4.1 ppm, —$C(=O)C\mathbf{H}_2$— at δ 2.33–2.28 ppm, and —$C(=O)CH_2C\mathbf{H}_2$— at δ 1.60 ppm. The peak areas of chemical shifts at 4.4 −4.2 ppm and at 4.2–4.0 ppm were equal, indicating that hydrolysis of the TAGs was avoided. Because the epoxidation of the terminal double bonds was not complete, the Green Polyols also showed chemical shifts of the remaining terminal double bonds (—$C\mathbf{H}$=CH_2 at 5.8 ppm, and —CH=$C\mathbf{H_2}$ at 5.0–4.8 ppm). The formic acid units on the backbone (chemical shift at δ 8 ppm) were presented in B1- and B2-Polyols but not in B3- and B4-Polyols, similar to their starting epoxides. The RTDB (mol %) of the Green Polyols and the number of formic acid units per TAG polyol are listed in Table III.

The solvent free synthetic strategy adapted (see synthesis section) was very successful for the synthesis of Green Polyols with controlled OH values. It was also confirmed in the ^{1}HNMR characterization of the epoxides and polyols that the controlled reaction parameters such as T_{ini}^{Epx} and T_R^{Epx} (see Table I) facilitated the avoidance of formic acid units attached on the epoxide backbone in batches B3 and B4. Also the polyols produced from the resultant epoxides such as B3-Green Polyol and B4-Green Polyol was completely free from formic acid residuals. The Green Polyols presented OH values between 83 and 119 mg KOH g— (Table III) and very low acid values, except for B1-Green Polyol which displayed a relatively high acid value due to its longer epoxidation reaction time. Although the OH values achieved using the green route are relatively lower compared to those of the PMTAG Polyols prepared previously with solvents,[30] they are large enough to make suitable monomers for the preparation of flexible as well as rigid foams. B3- and B4-Green Polyols which displayed very low acid values, no formic acid attached and significantly different OH values (83 and 119 mg KOH g^{-1}, respectively) were chosen for further physical characterizations, and used for the preparation of rigid and flexible polyurethane foams.

The GPC curves of the B3- and B4-Green Polyols are shown in Figure 1. The corresponding GPC data are listed in Table IV. The GPC revealed the presence of relatively important levels of

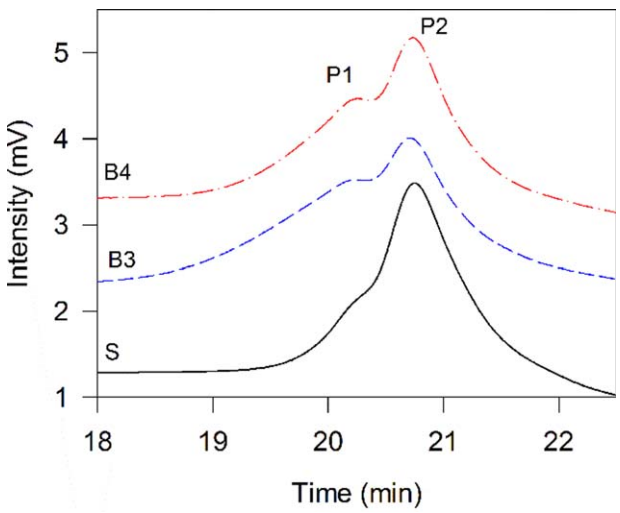

Figure 1. GPC chromatogram of Green Polyols. B3 and B4: B3- and B4-Green Polyol, respectively. S: GPC curve of the PMTAG polyol synthesized using solvents (standard PMTAG Polyol[30]) is provided for comparison purposes. [Color figure can be viewed in the online issue, which is available at wileyonlinelibrary.com.]

Table IV. Area % of Peaks P1 and P2 from GPC

Polyols	Peaks	Area %	Oligomers
B3-Green polyol	[a]P1	45	45%
	[b]P2	54	
B4-Green polyol	P1	37	37%
	P2	63	
PMTAG polyol	P1	13	13%
	P2	87	

P1: [a]M_n: 4437 g mol^{-1} and [b]M_w: 7030 g mol^{-1}, P2: M_n: 721 g mol^{-1}, and M_w: 1463 g mol^{-1}).

oligomers in the polyols. B3- and B4-Green Polyols comprised 45 and 37% oligomers, respectively, compared to 13% oligomers in the polyol synthesized using solvents (curve S in Figure 1). These include high molecular weight oligomers (M_w: 7030 g mol^{-1}) as well as low molecular weight oligomers (M_w: 1463 g mol^{-1}). The higher oligomerization during the solvent free reaction was due to a higher reaction temperature (85 °C compared to 25 °C).[31]

The composition of the PMTAG Green Polyols was determined with the help of ^{1}H NMR and HPLC analyses of the column chromatographic fractions of B4-Polyol. Seven different fractions (labelled F1 to F7) were obtained with ethyl acetate and hexanes as the solvents. Column chromatography, ^{1}H NMR and HPLC data are provided in the Supporting Information in Table SIV.

The ^{1}HNMR of F1 did not present the chemical shift at 3.6–3.2 ppm which is related to OH groups indicating that it is not the hydroxyl derivative. Also, F1 presented ~24 mol % unreacted terminal double bonds. F2 and F3 presented hydrolyzed TAG structures formed during the hydroxylation reaction. The ^{1}HNMR of F4, F5, and F6 presented chemical shifts at δ 5.3–5.2 ppm and 4.4–4.1 ppm of -CH_2C**H**(O)CH_2— and —OC**H**$_2$ CH(O)C**H**$_2$O— of the glycerol skeleton, respectively, and at δ 3.8–3.4 ppm of the proton neighboring hydroxyl groups indicating the presence of TAG diols and TAG tetrols. F4, F5 and F6 presented also some unreacted terminal double bonds (~10 mol %) as revealed by the chemical shifts at 4.8–5.0 ppm. Fraction F7 presented only tetrols (as revealed by the chemical shift at δ 3.8–3.4 ppm Figure S2 Supporting Information), with ~15 mol % unreacted terminal double bonds.

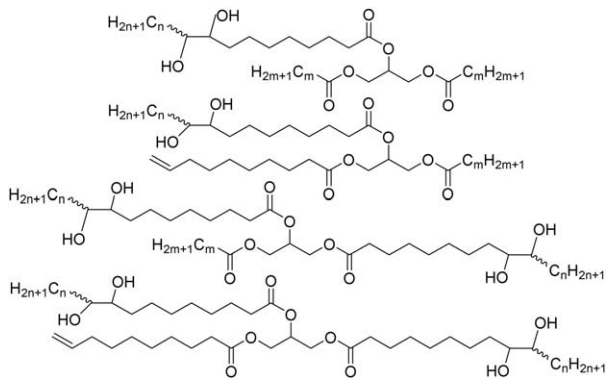

Scheme 2. General structures in PMTAG Green Polyol (n = 0, 2, 8; m = 11 to 20).

The ^{1}H NMR results were confirmed and complemented by HPLC. The general structures of the green polyols resulting from these analyses and based on structures of PMTAG itself[30] are presented in Scheme 2.

Physical Properties of PMTAG Green Polyols

Thermogravimetric Analysis of Green PMTAG Polyols. As indicated by the DTG profiles of B3- and B4-Green Polyols shown in Figure 2, B3- and B4-Green Polyols presented similar traces indicating a two-step degradation process. The large DTG peak at ~380 °C (TD1 in Figure 2) is associated with the breakage of the ester bonds.[32] This dominant step which was initiated at 240 °C and concluded at ~−420 °C involved ~60% of weight loss. The small DTG shoulder peak at ~450 °C (TD2, in Figure 2) is related to the decomposition of the ester groups and other fragments, and the degradation of the remaining carbonaceous materials from the previous step.[33] The onset of degradation of B3- and B4-Green Polyols as determined at 10% weight loss ($T^d_{10\%}$) was higher than 310 °C, indicating a good thermal degradation stability for the Green Polyols, comparable to other vegetable based polyols. Note that $T^d_{10\%}$ of B4-Green Polyol was relatively smaller compared to B3-Green Polyol (12 °C lower) probably due to the loss of terminal hydroxyls which content is higher in B4-Green Polyol.[33]

Crystallization and Melting Behavior of PMTAG Green Polyols. The crystallization and heating profiles (both at 5 °C min^{-1}) of B3- and B4-Green Polyols are shown in Figure 3(a,b), respectively. The corresponding thermal data is listed in the Supporting Information in Table SV. as can be seen in Figure 3, B3- and B4-Green Polyols present similar crystallization and heating behaviors with marked separation of a high and low temperature events inherited from the PMTAG similarly to the PMTAG Polyol synthesized via solvent mediation.[30] The difference between B3- and B4- Green Polyol manifested in a small difference in their onset temperature of crystallization (26 and

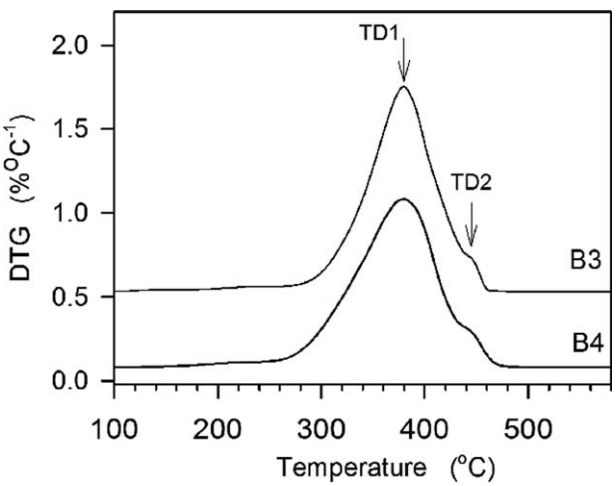

Figure 2. DTG profiles of B3- and B4-Green Polyols.

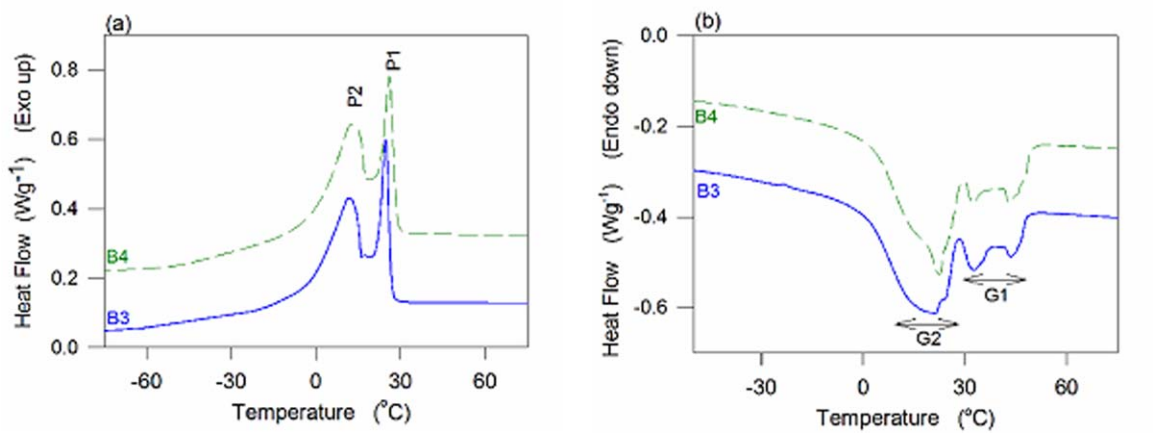

Figure 3. DSC thermograms of B3-, and B4-Green Polyols obtained during (a) Cooling, and (b) subsequent heating (5 °C min^{-1}). [Color figure can be viewed in the online issue, which is available at wileyonlinelibrary.com.]

29 °C, respectively) and offset temperature of melting (48 and 50 °C, respectively). Note that these values are consistent with the fact that B3-and B4-Green Polyols were not liquid at ambient temperature. The large difference in their OH values was not reflected in either the crystallization or melting traces, indicating that other structural attributes such as remaining double bonds and short chain moieties played a counter effect. The melting point of the Green Polyols as determined by the offset temperature of melting is ~2 °C higher than what was measured for the PMTAG Polyol synthesized via solvent mediation.[30] This may be due to the higher percentage of oligomers in the Green Polyols.

The heating thermogram of the Green Polyols displayed two groups of endothermic events [G2 below 30 °C, and G1 above 30 °C in Figure 3(b)] corresponding to the melting of a high and low melting portions of the polyols. the enthalpy of melting of G1 and G2 (~26 and ~66 J g^{-1}, respectively) was very similar to the enthalpy of P1 and P2, respectively, suggesting that they are effectively the recording of the melting of the "high" and "low" melting portions of the polyol, respectively. These DSC data indicate that with careful processing, it is possible to separate PMTAG Polyol into two fractions: one mainly constituted of low melting components, and another mainly constituted of high melting components. It is expected that at ambient temperature, one fraction will be solid and the other will remain liquid.

Flow Behavior and Viscosity of B3- and B4-Green Polyols. The shear stress versus shear rate at selected temperatures and viscosity versus temperature curves recorded for B3-, B4-Green Polyols are provided in the Supporting Information in Figures S2 and S3, respectively.

The fits to the Herschel–Bulkley model [eq. (1)] of the share rate–shear stress were linear ($R^2 > 0.99999$) for the entire shear rate range at temperatures from 40 °C to 90 °C for B3-Green Polyol and at temperatures from 50 to 90 °C for B4-Green Polyol indicating Newtonian behavior. Application of eq. (1) generated power index values (n) close to unity and no yield stress. The deviation from the Newtonian behavior above 200 s^{-1} at 30 °C for B3-Green Polyol and above 400 s^{-1} at 40 °C for B4-Green Polyol is due to the close proximity to the onset temperature of crystallization. Because their onsets of crystallization are closer than the temperatures at which their flow was Newtonian, the difference in flow behavior between B3-and B4-Green Polyols is attributed to the difference in OH value and terminal hydroxyls content which were higher in B4-Green Polyol.

The viscosity versus temperature curves of B3- and B4-Green Polyols presented the typical exponential behavior of liquid hydrocarbons.[34,35] The viscosity of the B4- Green Polyol was higher than that of B3-Green Polyol at all temperatures due to a higher number of hydroxyl groups which increases the polarity and intermolecular attractive force between the molecules by hydrogen bonding.[36] The Green Polyols presented a slightly higher viscosity than the Polyol prepared from PMTAG by solvent mediated reactions.[30] This difference is explained by the larger amount of oligomers in the B3- and B4-Green Polyols (37 and 45%, respectively) compared to PMTAG Polyol (13%).

Polyurethane Foams

One rigid and one flexible foam were prepared from B3- and B4-Green Polyols using a previously reported polymerization method.[27] Note that the catalyst amount for the flexible foam formulation (0.5 parts, see Table II) was chosen to avoid the cracks observed during the compression of the flexible foams made with smaller catalyst concentrations. The pictures of the rigid and flexible foams from B3-and B4-Green PMTAG Polyols shown in Figure 4, indicate that the polyurethane foams presented a smooth surface and a light yellow color.

As can be seen in Table V listing the cream time, gel time and rise time, the rigid foams formed relatively faster than the flexible foams. The difference in foaming reactivity is related to the presence of the extra catalyst and co-catalyst (additional 1 part of both, see Table II) and the highly reactive glycerol in the rigid foam formulation. The higher catalyst concentration in the formulation of the rigid foams enabled shorter mix times in the rigid foams compared to the flexible foams. Furthermore, the

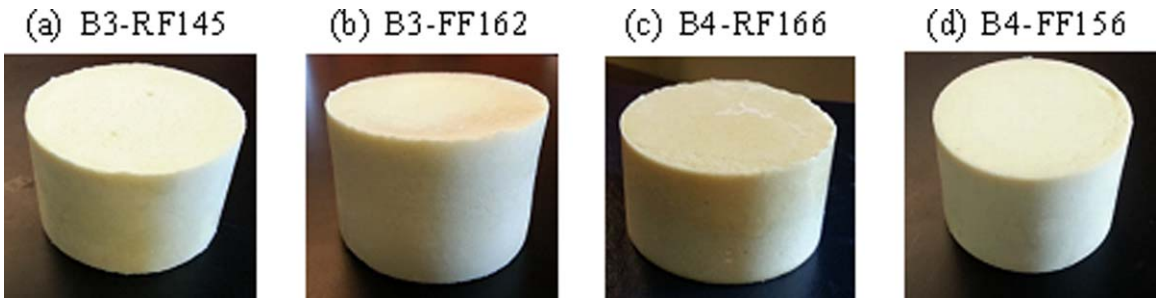

Figure 4. Pictures of rigid and flexible foams from B3-and B4-Green PMTAG Polyols. (a) B3-Green Polyol rigid foam of density 145 kg m^{-3} (B3-RF145), (b) B3-Green Polyol flexible foam of density 162 kg m^{-3} (B3-FF162), (c) B4-Green Polyol rigid foam of density 166 kg m^{-3} (B4-RF166) and (d) B4-Green Polyol flexible foam of density 156 kg m^{-3} (B4-FF156). [Color figure can be viewed in the online issue, which is available at wileyonlinelibrary.com.]

presence of the glycerol in the rigid foam formulation speeded the entire polymerization reaction and drove the crosslinking reaction.

FTIR of B4-Green Polyol Foams. The FTIR spectra of the rigid and flexible foams produced from both B3- and B4-Green Polyol confirmed the formation of urethane linkages. As shown in Figure 5, representing the FTIR spectra of B4-flexible and a rigid foams typical of all the foams, the characteristic absorption band of NH groups, C═O and C─N bonds which are associated with the urethane linkage were presented at 3300–3400 cm^{-1}, 1700 cm^{-1}, and at 1516 cm^{-1}, respectively.[37,38] However, as indicated by the weak band at 2270 cm^{-1} of the NCO group, some of the isocyanate did not react with the polyol.[15,37] The overlapping peaks between 1710 and 1735 cm^{-1} suggest the presence of urea and isocyanurates in the foams. The peak at ~1410–1420 cm^{-1} reveals the presence of isocyanurate trimers, indicating the occurrence of trimerization reactions of the diisocyanates during the foaming process. The stretching bands of the ester groups are particularly visible at 1744 cm^{-1} (C═O), 1150–1160 cm^{-1} (O─C─C) and 1108–1110 cm^{-1} (C─C(═O) ─O). The stretching vibration of ─C─H in $─CH_3$ and $─CH_2$ groups in the aliphatic chains are also visible at 2917–2925 cm^{-1}, and 2850 cm^{-1} respectively.[39] The CH_2 stretching vibration and CH_2 bend are also clearly visible at 2800–3000 cm^{-1} and 1030–1050 cm^{-1}, respectively.[15]

SEM Analysis of Green Polyol Foams. Figure 6(a–d) show SEM images of the rigid and flexible foams prepared from B4- and B3-Green Polyol, respectively. The cell structures of Figure 6(a–d) are typical of all the rigid and flexible foams prepared in the present work. The characteristics of the cell structure such as number and size of the cells was determined from the analysis of all the visually separate cells of at least two specimens of each foam. The values provided here are the subsequent calculated average and standard deviations. The Green Polyol rigid foam displayed compact and uniformly distributed cells (B4: 450 ± 44 μm, B3: 475 ± 60 μm). On the other hand, although with a somewhat similar average cell size (B4: 494 ± 145 μm, B3: 500 ±190 μm) the Green Polyol flexible foam presented a heterogeneous cell structure with cell size ranging from 277 to 784 μm for B4 and 200 to 800 μm for B3. The stark differences in cell structure between the rigid and flexible foams is attributable to the compounded effects of high cross linking density achieved by the addition of glycerin in the rigid foam formulation and the different rates of crosslinking of terminal and internal hydroxyls in the Green polyol flexible foam formulation.[40] Because both rigid and flexible foams only contain closed cells, they may also have applicability in thermos insulation applications.

Both the rigid and flexible foams prepared from the PMTAG Green Polyols displayed a smaller number of cells and larger cell size than the rigid and flexible foams from PMTAG Polyol prepared via solvent mediation.[27] Beside the OH value and terminal OH group effects considerations (OH value 119 mg KOH g^{-1} and 18.3% terminal hydroxyl in the B4-Green Polyol for example vs. OH value of 155 mg KOH g^{-1} and 24.1% terminal hydroxyl groups in the polyol prepared via solvent

Table V. Reactivity Profile for the Processing of Green Polyol Rigid and Flexible Foams

	Cream time (s)	Gel time (s)	Rise time (s)
Rigid foam	6-10	28-32	72-74
Flexible foam	15-20	31-35	75-80

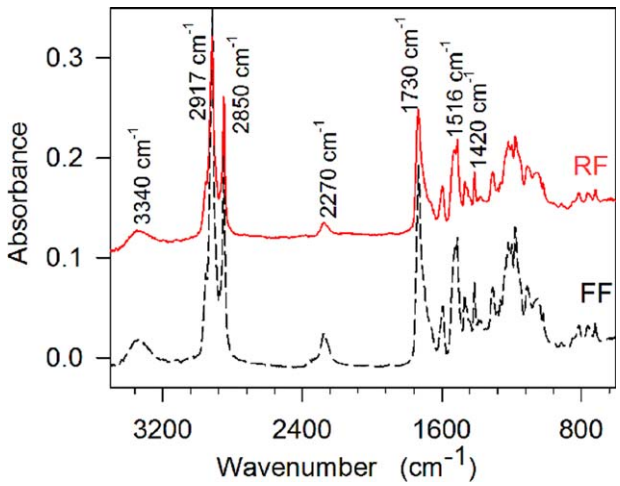

Figure 5. Typical FTIR spectra of rigid (RF) and flexible (FF) B4-Green Polyol foam. [Color figure can be viewed in the online issue, which is available at wileyonlinelibrary.com.]

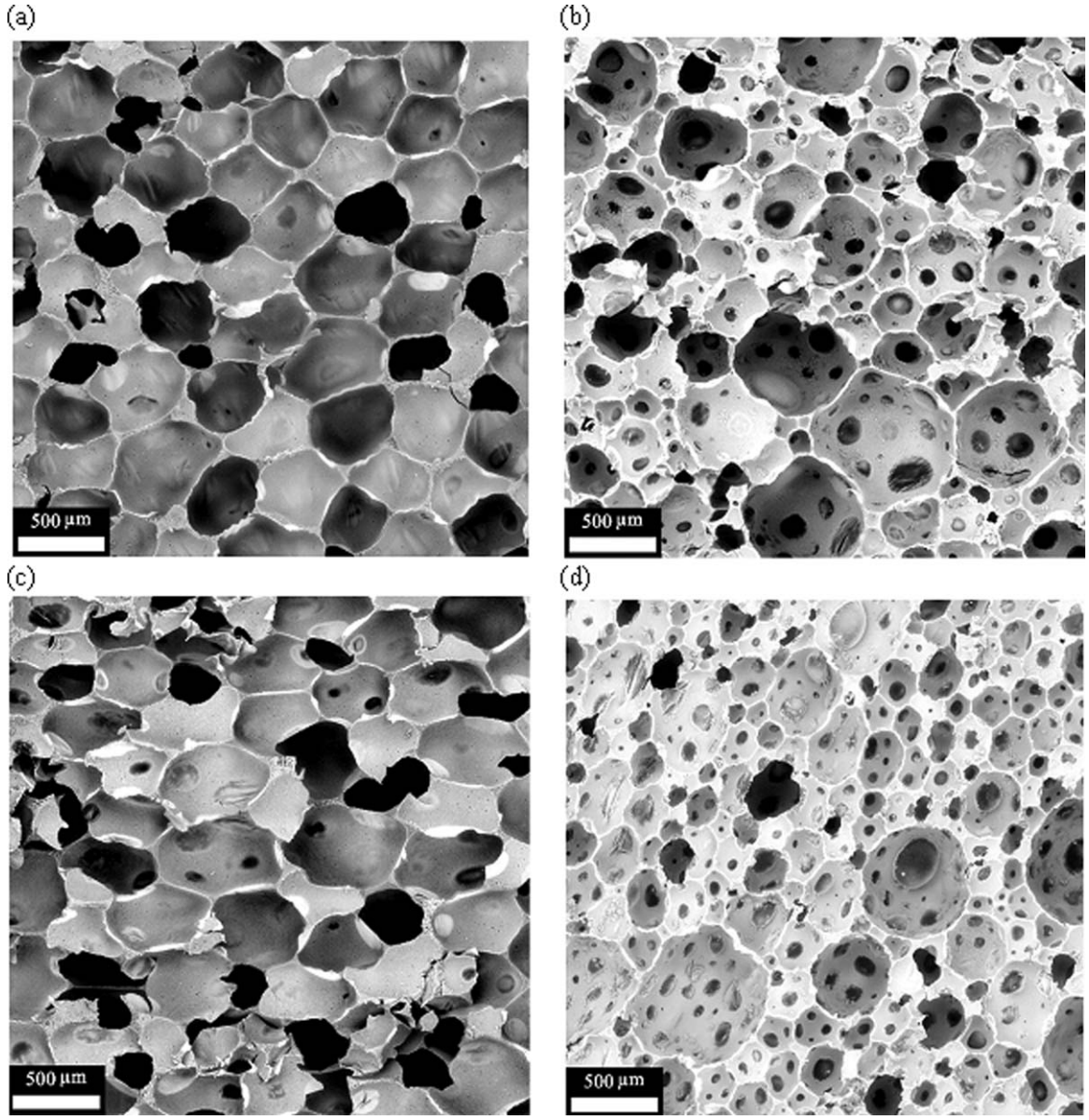

Figure 6. SEM micrographs of (a) B4-Green Polyol rigid foam, (b) B4-Green Polyol flexible foam, (c) B3-Green Polyol rigid foam and (d) B3-Green Polyol flexible foam.

mediation), the larger amount of oligomers in the Green Polyol (37% in B4-Green Polyol) may have added an extra contribution for the larger size of cells of the rigid and flexible Green Polyol foams.

Thermal Stability of PMTAG Green Polyol Foams. As exemplified in Figure 7 showing the DTG profiles of B4-Green Polyol rigid and flexible foams, the foams produced with the Green Polyols degraded following a multi stage process. The first peak centered at 296–300 °C (T_{D1} in Figure 7) is related to the dissociation of urethane bonds that has taken place either through the dissociation of the isocyanate and alcohol or to the formation of primary or secondary amines, olefin and carbon dioxide.[41,42] This first step involved a total weight loss of ~12–17%. The second and third decomposition steps signaled with the DTG peaks at ~370 and 420 °C (T_{D2} and T_{D3} in Figure 7) are associated with the decomposition of the soft segments.[42] The soft segment (polyol back bone) dissociates into carbon monoxide, carbon dioxide, carbonyls (aldehyde, acid, acrolein) olefins and alkenes.[32,42] These two decomposition steps involved the largest loss with 65–80% of the total weight. The last step of degradation is signaled with the DTG peak at ~460 °C (T_{D4} in Figure 7) and is related to the decomposition of more strongly bonded fragments associated with the polyol backbone that occur at high temperature, and probably to the degradation of remaining carbonaceous materials from the previous step.

Note that the onset temperature of degradation of the rigid foam whether determined at 5 or 10% weight loss was consistently lower (~16 °C) than that of the flexible foams. This can

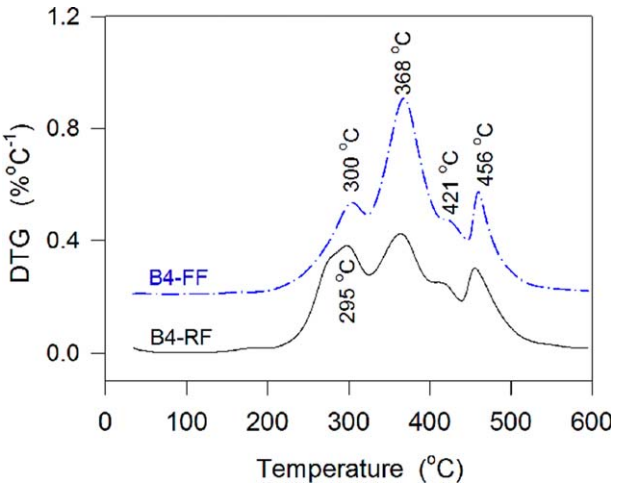

Figure 7. DTG curves of B4-Green Polyol rigid foam (B4-RF) and B4-Green Polyol Flexible Foam (B4-FF). [Color figure can be viewed in the online issue, which is available at wileyonlinelibrary.com.]

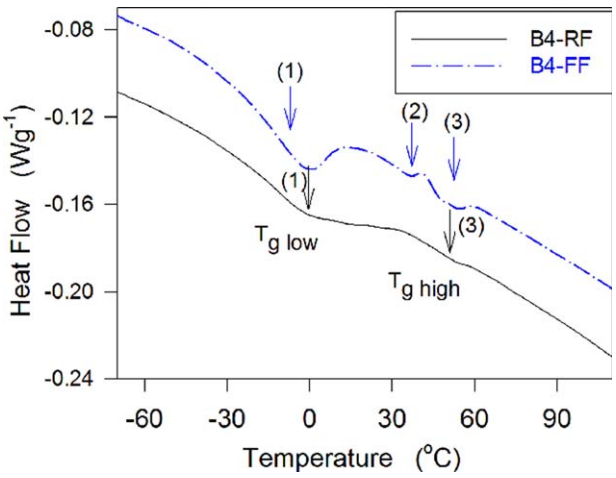

Figure 8. DSC heating thermogram (2nd cycle) of the B4-Green Polyol rigid (B4-RF) and flexible foams (B4-FF): arrow 1 indicates $T_{g_{low}}$, arrow 2 indicates $T_{g_{int}}$ and arrow 3 indicates $T_{g_{high}}$. [Color figure can be viewed in the online issue, which is available at wileyonlinelibrary.com.]

be due to the degradation of short chain urethane structures from the glycerin crosslinker.

Thermal Transition of Green Polyol Foams. DSC analysis was carried out on the rigid and flexible foams produced with B4-Green Polyol to study the thermal phase transition behavior of the Green Polyol foams. Figure 8 shows the DSC profiles obtained during the second heating cycle of rigid and flexible B4-Green Polyol foams respectively. One can notice that the thermogram of rigid B4-Green Polyol foam presents two inflection points indicating two glass transitions ($T_{g_{low}}$ (arrow 1 in Figure 9) at ~−12 °C and $T_{g_{high}}$ (arrow 2 in Figure 9) at ~49 °C of B4-RF in Figure 8) whereas B4-Green Polyol flexible foam thermogram shows three inflection points indicating three glass transitions ($T_{g_{Low}}$ at −11 °C, $T_{g_{int}}$ at ~34 °C and $T_{g_{high}}$ at ~46 °C of B4-FF, arrow 1, 2, and 3 in Figure 8).

$T_{g_{high}}$ of both the rigid and flexible Green Polyol Foams is attributable to the relaxation of the urethane segments and their $T_{g_{low}}$ to the molecular motion of the soft segments related to the polyols.[43] The glass transition observed at intermediate temperature ($T_{g_{int}}$) in the flexible Green Polyol Foam is probably due to the relaxation of the short chain urethane segments resulting from the Green Polyol mixture.

Compressive Strength of Green Polyol Foams. The compressive strength of rigid foams prepared from B3-Green Polyol (density 145 kg m^{-3}, B3-RF145), and B4-Green Polyol (density 166 kg m^{-3}, B4-RF166), and flexible foams from B3-Green Polyol (B3-FF162, density 162 kg m^{-3}), and B4-Green Polyol (B4-FF156, density 156 kg m^{-3}) was characterized by the compressive stress-strain measurements. Figure 9(a,b) show the compressive strength versus strain curves of the examined rigid and flexible Green Polyol foams, respectively. The rigid and flexible foams displayed relatively quick yielding followed by a plateau-like region over which there was a little increase in stress with

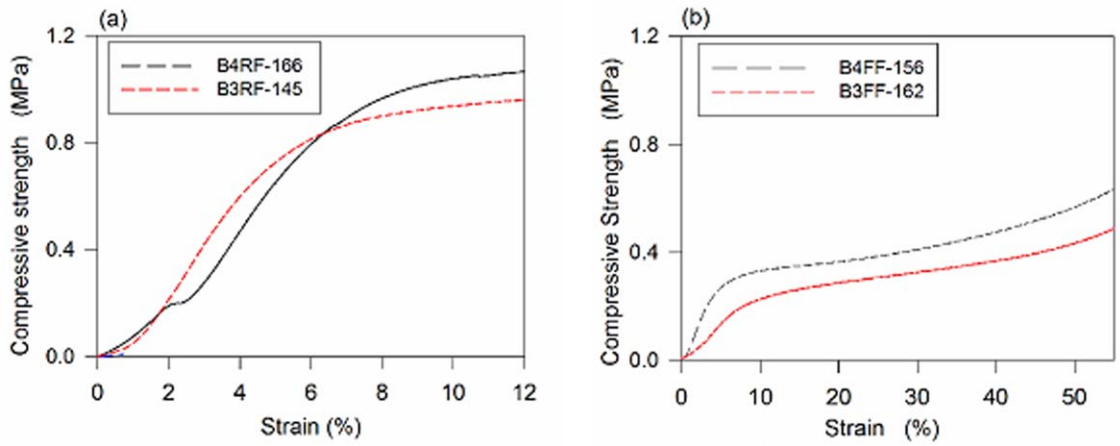

Figure 9. Compressive strength versus strain curves of (a) Rigid foams: B3-RF145 (B3-Green Polyol rigid foam of density 145 kg m^{-3}), B4-RF166 (B4-Green Polyol rigid foam of density 166 kg m^{-3}) (b) Flexible foams. B3-FF162 (B3-Green Polyol flexible foam of density 162 kg m^{-3}), B4-FF156 (B4-Green Polyol flexible foam of density 156 kg m^{-3}). [Color figure can be viewed in the online issue, which is available at wileyonlinelibrary.com.]

Table VI. Compressive Strength of Rigid Foams: B4-RF166 (B4-Green Polyol Rigid Foam of Density 166 kg m^{-3}) versus RF-165 (PMTAG Polyol Rigid foam of Density 165 kg m^{-3}) at 6 and 10% Deformation

Foams	Density (kg m^{-3})	Compressive strength (MPa)		Recovery %: after 48 h
Rigid Foams				-
@ Strain (%)		6	10	-
B3-RF145	145	0.79	0.94	-
B4-RF166	166	0.72	1.05	-
RF	165	0.66	0.85	-
Flexible Foams				-
@ Strain (%)		10	25	-
B3-FF162	162	0.21	0.30	94
B4-FF156	153	0.33	0.38	92
FF-156	156	0.69	0.88	80

Flexible foams: B3-FF162 (B3-green polyol flexible foam of density 162 kg m^{-3}), B4-FF156 (B4-Green Polyol flexible foam of density 156 kg m^{-3}), and FF-156 (PMTAG Polyol flexible foam of density 156 kg m^{-3}) at 10 and 25% deformation.

increase in strain. The elastic region was ~4% in the case of rigid foams and 6% in case of flexible foams. Each region is determined by a specific mechanism of deformation. Linear elasticity is controlled by cell wall bending, and, in the case of closed cells such as in the case of the present foams, by stretching of the cell walls.[39] The plateau-like region [above ~8% for the rigid foams in Figure 9(a) and between 10 to 30% for the flexible foams in Figure 9(b)] results from either the collapse or cell wall buckling of the foams.[39] Further compression of the flexible foams above 30% resulted in an irreversible damage to the cell walls and is called the densification region.[39]

Table VI lists the compressive strength of rigid foams at 6 and 10% deformation and that of the flexible foams at 10 and 25% deformation. Even though both the B3- and B4-Green Polyol rigid foams were prepared based on a total OH value of 450 mg KOH g^{-1}, their compressive strength values were slightly different. The B3- and B4-Green Polyols rigid foams displayed a higher compressive strength compared to PMTAG Polyol rigid foam.[27] This may be due to the extra amount of highly reactive glycerol cross linker added for the rigid foam formulation of B3- and B4-Green Polyol rigid foams to make for the targeted OH value of 450 mg KOH/g. Four (4) and two (2 parts) of extra glycerol on top of what was added to PMTAG Polyol were needed for the B3- and B4-Green Polyols, respectively, to attain the same target OH value of the rigid foam formulations (see Table II).

The compressive strength value of the rigid foams obtained from B3- and B4-Green Polyols are higher than those prepared from natural TAG oil polyols such as, soybean oil polyol[2] and canola oil polyol.[2] For example, the rigid B3- and B4-Green polyol foams presented compressive strengths that are three (3) times larger than the 0.32 MPa of the rigid foams prepared with polyol from soybean oil with the same density (~160 kg m^{-3}), understandably because the B3- and B4-Green polyols have lesser dangling chains and relatively large amounts of primary hydroxyl groups contrary to the soybean oils which presented internal hydroxyl groups only.

B3FF-162 and B4FF-156 displayed a significantly lower compressive strength than the flexible foam of similar density 156 kg m^{-3} made from PMTAG Polyol. This is due to the more marked effect of the difference in OH value of B3- and B4-Green Polyol (B3: 83 mg KOH g^{-1} and B4: 119 mg KOH g^{-1} compared to 155 mg KOH g^{-1} for PMTAG Polyol and lesser percentage of terminal hydroxyls (B3: 16.5 mol % and B4: 18.3 mol % compared to 24.1 mol %) which become significant in the absence of the added glycerol.

The recovery in thickness of the flexible foam made from B4-Green Polyol (B4FF-156) was measured after 65% compression at suitable times using a Vernier caliper. The results are presented in Figure 10. As can be seen in the Figure 10, B4FF-156 recovery was very fast reaching >80% in <2 min and ~90% after 5 min. These values are 10% higher than those achieved by the same density flexible foam produced with PMTAG Polyol. The difference in flexibility between B4FF-156 and PMTAG Polyol flexible Foam (Table VI), as elucidated by the compressive strength and recovery data, can be related to the differences in OH value and lesser percentage of terminal hydroxyls in their corresponding polyol structure. This indicates the compressive strength and the flexibility of the flexible foams can be controlled to a relatively large extent by controlling the OH value and the terminal hydroxyls of the polyol.

The properties of the Green Polyol flexible foams also compare favorably with the commercial and biobased flexible foams. Although the flexible foam industry relies on petroleum based polyols such as poly ether polyols,[9,44] lipid-based polyol are increasingly used, particularly as blends such as soy-castor oil-based polyol,[45] rapeseed polyol,[46] soy polyol,[9,28] palm oil polyol.[44]

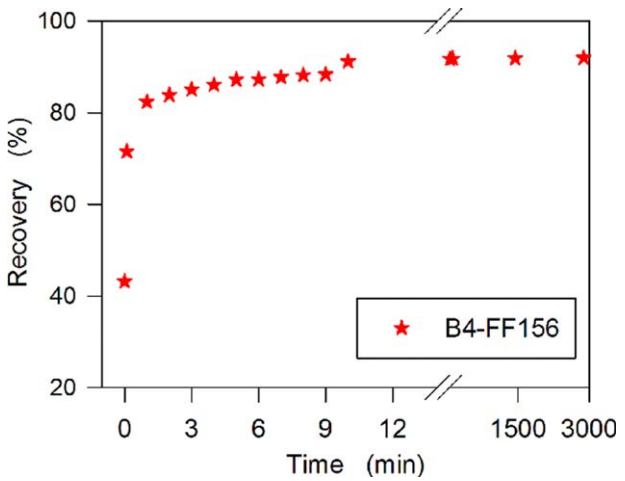

Figure 10. Recovery (%) in thickness of B4-FF156 (B4-Green Polyol flexible foam of density 156 kg m^{-3}) versus time. [Color figure can be viewed in the online issue, which is available at wileyonlinelibrary.com.]

The flexible foams of the present study present compressive strengths that are in the 0.1–0.4 MPa range displayed by these foams. The comparison the overall properties of the flexible foams of the present work with those materials suggest that the Green Polyols would be very interesting as blend with commercial petroleum polyols and would provide highly functional flexible foams. One would expect similar or better results than what was achieved with palm oil polyol for which a 15% substitution with Alfapol, a petroleum based polyether polyol, enhanced the compressive strength by ~60%[44] or soy oil polyol where a 30% substitution caused 50% improvement in compressive strength.[9] The partial replacement commercial petroleum based polyols with the Green Polyols of the present work in fact show great promise for both flexible and rigid applications.

CONCLUSIONS

Green Polyols with controlled OH value and primary hydroxyls were successfully synthesized from the product of the metathesis of palm oil (PMTAG) using an alternative, solvent free epoxidation and hydroxylation pathway. The solvent free method has been demonstrated to yield very versatile green polyols comprised of diol and tetrol terminal groups and having hydroxyl values as high as 119 mg KOH g^{-1}. The structures of the polyols were determined by the structures of the feedstock and dramatically influenced by the reaction conditions. It has been shown that the polyol hydroxyl value can be controlled to some extent by the reaction conditions. It has also been demonstrated that the formic acid moieties that attach to the polyol backbone under specific reaction conditions can be avoided by adequately tuning the time and temperature of the epoxidation reaction. Although presenting a relatively large number of oligomeric material (~45%), the Green Polyols presented melting temperatures (~48 °C) and viscosity profiles that are very manageable for preparing flexible as well as rigid foams.

Two designer polyols (so-called B3- and B4-Green Polyols) having OH values of 83 and 119 mg KOH/g, respectively, and 16 and 18% primary hydroxyls, respectively, were fully characterized and used to produce very functional rigid as well as flexible foams. Both the Green Polyol Rigid and Flexible Foams displayed high onsets of decomposition (270 °C) indicating good thermal stability comparable to other lipid based polyols. The compressive strength of the Green Polyol Rigid Foams compare favorably with those previously prepared from PMTAG via solvent mediation. The Green Polyol Flexible foams presented even higher recovery (94%) coupled with a relatively a low and tunable compressive strength because of the larger range of control of the structures of the Green Polyols and larger oligomer content compared to the polyol obtained by solvent mediated pathway. Furthermore, the closed cell structure of the foams as evaluated from SEM images, indicate that they are suitable for structural and thermal insulation applications. The findings of the present study, particularly the results obtained with the flexible foams, bode well for the success of the strategy based on a green economical synthetic route for the production of polyols from vegetable oil based feedstocks.

ACKNOWLEDGMENTS

The authors thank the Grain Farmers of Ontario, Elevance Renewable Sciences, Trent University, the GPA-EDC, Ontario Ministry of Agriculture, Food and Rural Affairs, Industry Canada and NSERC for financial support. They also thank Dr. Michael Floros for his kind help in taking SEM Pictures. Author Contributions: Prasanth S. Pillai is the lead author of this manuscript and has contributed towards research design and also conducted the experimental work to acquire data, analyze and interpret it under Professor Suresh S. Narine's supervision. Prasanth .S. Pillai has also written the manuscript with critical input from Prof. Suresh Narine, Dr. Laziz Bouzidi and Dr. Shaojun Li. Furthermore, Dr. Shaojun Li and Dr. Laziz Bouzidi has contributed to the review of the chemical and physical characterization of rigid and flexible polyurethane foams.

REFERENCES

1. Randall, D.; Lee, S. The Polyurethanes Book; Huntsman Polyurethanes: Belgium, **2002**.
2. Narine, S. S.; Kong, X.; Bouzidi, L.; Sporns, P. *J. Am. Oil Chem. Soc.* **2007**, *84*, 65.
3. Somani, K. P.; Kansara, S. S.; Patel, N. K.; Rakshit, A. K. *Int. J. Adhes. Adhes.* **2003**, *23*, 269.
4. Velayutham, T. S.; Majid, W. H. A.; Ahmad, A. B.; Kang, G. Y.; Gan, S. N. *Prog. Org. Coat.* **2009**, *66*, 367.
5. General, **2013**. Polymer Foam Market By Types (Polyurethane, Polystyrene, Polyvinyl Chloride, Polyolefin, Phenolic, Melamine and Others), Applications (Packaging, Building & Construction, Furniture & Bedding, Automotive, Wind Energy and Others) & Geography - Global Trends & Forecasts to 2018. marketsandmarkets CH 1465.
6. Szycher, M. Szycher's Hand Book of Polyurethanes; Cardio-Tech International Inc.: Woburn, MA (US), **1999**.
7. Guan, J.; Song, Y.; Lin, Y.; Yin, X.; Zuo, M.; Zhao, Y.; Tao, X.; Zheng, Q. *Ind. Eng. Chem. Res.* **2011**, *50*, 6517.
8. More, A. S.; Gadenne, B.; Alfos, C.; Cramail, H. *Polym. Chem.* **2012**, *3*, 1594.
9. Zhang, L.; Jeon, H. K.; Malsam, J.; Herrington, R.; Macosko, C. W. *Polymer* **2007**, *48*, 6656.
10. Tan, S.; Abraham, T.; Ference, D.; Macosko, C. W. *Polymer* **2011**, *52*, 2840.
11. Khoe, T. H.; Otey, F. H.; Frankel, E. N. *J. Am. Oil Chem. Soc.* **1972**, *49*, 615.
12. Hu, Y. H.; Gao, Y.; Wang, D. N.; Hu, C. P.; Zu, S.; Vanoverloop, L.; Randall, D. *J. Appl. Polym. Sci.* **2002**, *84*, 591.
13. Babb, D. A. In Synthetic Biodegradable Polymers; Springer: Advances in Polymer Science, **2012**.
14. Potts, J.; Lynch, M.; Wilkings, A.; Huppe, G.; Cunningham, M.; Voora, V. The State of Sustainability Initiatives Review 2014: Standards and the Green Economy; International Institute for Sustainable Development (IISD) and the International Institute for Environment and Development (IIED), **2014**, 332.

15. Narine, S.; Yue, J.; Kong, X. *J. Am. Oil Chem. Soc.* **2007**, *84*, 173.
16. Zlatanic, A.; Petrovic, Z. S.; Dusek, K. *Biomacromolecules* **2002**, *3*, 1048.
17. Rybak, A.; Fokou, P. A.; Meier, M. A. R. *Eur. J. Lipid Sci. Technol.* **2008**, *110*, 797.
18. Mol, J. C.; Buffon, R. *J. Braz. Chem. Soc.* **1998**, *9*, 1.
19. Thomas, R. M.; Keitz, B. K.; Champagne, T. M.; Grubbs, R. H. *J. Am. Chem. Soc.* **2011**, *133*, 7490.
20. Malacea, R.; Dixneuf, P. H. In Green Metathesis Chemistry; Springer, Green Metathesis Chemistry; Part of the Series NATO Science for Peace and Security Series: Chemistry and Biology, **2010**, p 185.
21. Mol, J. *Top. Catal.* **2004**, *27*, 97.
22. Connon, S. J.; Blechert, S. *Angew. Chem. Int. Ed.* **2003**, *42*, 1900.
23. Rosenburg, D. W. U.S. Patent US4545941 A (**1985**).
24. Li, S. J.; Hojabri, L.; Narine, S. S. *J. Am. Oil Chem. Soc.* **2012**, *89*, 2077.
25. Tian, Q. P.; Larock, R. C. *J. Am. Oil Chem. Soc.* **2002**, *79*, 479.
26. Biermann, U.; Metzger, J. O.; Meier, M. A. R. *Macromol. Chem. Phys.* **2010**, *211*, 854.
27. Pillai, P. K.; Li, S.; Bouzidi, L.; Narine, S. S. *Ind. Crop. Prod.* **2016**, *83*, 568.
28. Zhang, C.; Xia, Y.; Chen, R.; Huh, S.; Johnston, P. A.; Kessler, M. R. *Green Chem.* **2013**, *15*, 1477.
29. Li, S.; Bouzidi, L.; Narine, S. S. *Ind. Eng. Chem. Res.* **2013**, *52*, 2209.
30. Pillai, P. K.; Li, S.; Bouzidi, L.; Narine, S. S. *Ind. Crop. Prod.* **2016**, *84*, 205.
31. Guo, A.; Cho, Y.; Petrović, Z. *S. J. Polym. Sci. A Polym. Chem.* **2000**, *38*, 3900.
32. Gryglewicz, S.; Piechocki, W.; Gryglewicz, G. *Bioresour. Technol.* **2003**, *87*, 35.
33. Lin, B.; Yang, L.; Dai, H.; Hou, Q.; Zhang, L. *J. Therm. Anal. Calorim.* **2009**, *95*, 977.
34. Goodrum, J. W.; Eiteman, M. A. *Bioresour. Technol.* **1996**, *56*, 55.
35. Eiteman, M. A.; Goodrum, J. W. *J. Am. Oil Chem. Soc.* **1994**, *71*, 1261.
36. Li, Y.; Sun, X. S.; Am, J. *Oil Chem. Soc.* **2014**, *91*, 1425.
37. Chuayjuljit, S.; Sangpakdee, T.; Saravari, O. *J. Metals Mater. Miner.* **2007**, *17*, 7.
38. Piszczyk, Ł.; Strankowski, M.; Danowska, M.; Hejna, A.; Haponiuk, J. T. *Eur. Polym. J.* **2014**, *57*, 143.
39. Gu, R.; Konar, S.; Sain, M. *J. Am. Oil Chem. Soc.* **2012**, *89*, 2103.
40. Campanella, A.; Bonnaillie, L. M.; Wool, R. P. *J. Appl. Polym. Sci.* **2009**, *112*, 2567.
41. Javni, I.; Petrović, Z. S.; Guo, A.; Fuller, R. *J. Appl. Polym. Sci.* **2000**, *77*, 1723.
42. Shufen, L.; Zhi, J.; Kaijun, Y.; Shuqin, Y.; Chow, W. *Polym. Plast. Technol. Eng.* **2006**, *45*, 95.
43. Tanaka, R.; Hirose, S.; Hatakeyama, H. *Bioresour. Technol.* **2008**, *99*, 3810.
44. Pawlik, H.; Prociak, A. *J. Polym. Environ.* **2012**, *20*, 438.
45. Zhang, C.; Kessler, M. R. *ACS Sustainable. Chem. Eng.* **2015**, *3*, 743.
46. Malewska, E.; Bąk, S.; Prociak, A. *J. Appl. Polym. Sci.* **2015**, *132*, 35, 42372(1–11).